Journal of Computational Physics 294 (2015) 191–207

Contents lists available at ScienceDirect

Journal of Computational Physics

www.elsevier.com/locate/jcp

Heat flux expressions that satisfy the conservation laws in atomistic system involving multibody potentials

Yao Fu *,[1], Jeong-Hoon Song *,[2]

Department of Civil, Environmental and Architectural Engineering, University of Colorado at Boulder, Boulder, CO 80309, United States

ARTICLE INFO

Article history:
Received 23 July 2014
Received in revised form 16 March 2015
Accepted 25 March 2015
Available online 31 March 2015

Keywords:
Atomistic–continuum
Multibody potential
Thermomechanical quantities
Conservation laws
Heat flux

ABSTRACT

Heat flux expressions are derived for multibody potential systems by extending the original Hardy's methodology and modifying Admal & Tadmor's formulas. The continuum thermomechanical quantities obtained from these two approaches are easy to compute from molecular dynamics (MD) results, and have been tested for a constant heat flux model in two distinctive systems: crystalline iron and polyethylene (PE) polymer. The convergence criteria and affecting parameters, i.e. spatial and temporal window size, and specific forms of localization function are found to be different between the two systems. The conservation of mass, momentum, and energy are discussed and validated within this atomistic–continuum bridging.

1. Introduction

The success of continuum mechanics on predicting material response and failure in the macroscopic length scale is undeniable. Accompanied with the development of new techniques of reducing feature size, the applicability of continuum mechanics to fine scale phenomena attracts increasing attention. There is a growing need to interpret continuum concepts and laws in terms of atomistic/molecular behaviors to extend the concepts of continuum mechanics such as stress and strain to nano-scale. Classical molecular dynamics (MD) simulations have been widely used to capture the microscopic behaviors with atomistic resolution. Even though classical MD cannot resolve the electronic degrees of freedom, which is critical for understanding chemical reactions, bond breaking, and some of other fundamental aspects of atomic interactions, it can address the interaction of up to millions of atoms with satisfying accuracy thus being well suited to investigate nano-scale phenomena [1–3]. In MD simulations, the trajectories of interacting atoms are computed based on Newton's laws of motion, where the force on each atom is obtained from the spatial derivative of the interatomic potential energy.

The atomistic variables retrieved from MD simulations have been attempted to interpret the continuum quantities, in order to enable the multiscale linkage between microscopic and macroscopic scales in either hierarchical or concurrent modeling [4–12]. Virial stress by Clausius [13] and Maxwell [14,15] is probably the first attempt to derive microscopic definitions of stress tensor through the so-called virial theorem. Virial stress has been widely used in atomistic simulations due to its simple form and ease of computation. Irving and Kirkwood [16] developed point-wise stress tensor and heat flux vector as a statistical average of atomistic variables in their classical paper on the equations of hydrodynamics. However,

* Corresponding authors.
E-mail addresses: Yao.Fu@colorado.edu (Y. Fu), JH.Song@colorado.edu (J.-H. Song).
[1] Post-doctoral Fellow.
[2] Assistant Professor.

http://dx.doi.org/10.1016/j.jcp.2015.03.050
0021-9991/

the definitions of stress and heat flux are difficult to implement in atomistic simulations because the formulation involves a series expansion of the Dirac delta function and the probability density distribution function of the dynamic ensemble which is usually not known *a prior*. In order to obtain the stress and heat flux fields from MD simulations of non-equilibrium systems, Hardy [17,18] established conservation laws in which continuum thermomechanical fields are defined in terms of atomistic quantities through a localization function. The so-called Hardy stress has arbitrary spatial resolution and is often used in atomistic simulations [19–22]. However, Hardy's formulation has been explicitly based on the assumption of pair interatomic potential. Zimmerman et al. [21,22] examined the conditions under which the formulas could be valid and extended Hardy's work to include embedded atom method (EAM) potentials. Chen [23] further attempted formulating the stress and heat flux expressions in Hardy's framework to include three-body potentials of the Tersoff type [24,25] and the Stillinger–Weber type [26]. Multibody potentials have been considered by Delph [27], who discussed the applicability of Hardy's approach in more general context. However, the ambiguity on how to distribute the total potential energy among the atoms still remains one of the difficulties to extend Hardy's formulation to general multibody potential systems.

Murdoch [28–32] developed stress and heat flux expressions in a similar manner with Hardy by directly taking spatial average of the atomistic equation of motion with a normalized weighting function. Note that, in this work, Murdoch also considered temporal averaging besides spatial averaging to identify the computed quantities with experimentally measured values that are local averages of molecular behaviors in both space and time. In contrast to Hardy's approach, Murdoch's approach does not explicitly restrict the type of interatomic potentials for the systems under study. However, the disadvantage is the multiple integration involved in the resulting expressions, which makes it comparably more computationally expensive to implement for MD simulations. Admal and Tadmor [33] adopted Murdoch's methodology to avoid the ambiguities of energy decomposition among the atoms. By conducting combined ensemble and spatial averaging, Admal and Tadmor developed stress and heat flux expressions suitable for atomistic modeling.

Due to the lack of consensus on the definitions of continuum thermomechanical quantities in terms of atomistic variables that satisfy the conservation equations, in this study, we will discuss and compare the thermomechanical expressions developed by different approaches, with special focus on the heat flux definitions from Hardy and Admal & Tadmor. In Section 2, we briefly recall Hardy's formalism and extend it to multibody potential systems in the similar manner as Delph [27]. The validity of the conservation of mass, momentum, and energy are examined in detail. In Section 3, the potential part of heat flux expression is proposed the same as Hardy's original formulae and that in Admal & Tadmor's work. The energy density expression can be derived from the conservation of energy and involves integration over time. In Section 4, constant heat flux MD models are established for a crystalline iron described by the EAM potential and a coarse-grained (CG) model of amorphous polyethylene (PE) polymer system which involves up to four-body potentials. The expressions from Hardy's and Admal & Tadmor's methodologies are employed to compute the heat flux vectors in the two systems. Balance of energy is also investigated numerically in Hardy's and Admal & Tadmor's frameworks.

2. Expressions of the thermomechanical quantities involving multibody potentials using Hardy's approach

Hardy's original work can be found in Refs. [17,18]. Here we apply a similar procedure to obtain the stress and heat flux expressions for multibody potential systems. The essence of Hardy's approach is to link the continuum and atomistic scales through a localization function, $\psi(\mathbf{x},t)$, which assigns weights to the atoms that contribute to the interested continuum quantities at the spatial point $\mathbf{x}$ and time t. Hardy defines mass density, $\rho(\mathbf{x},t)$, momentum density, $\mathbf{p}(\mathbf{x},t)$, and energy density, $e^h(\mathbf{x},t)$, as follows:

$$\rho(\mathbf{x},t) := \sum_i m^i \psi\left(\mathbf{r}^i - \mathbf{x}\right) \tag{2.1a}$$

$$\mathbf{p}(\mathbf{x},t) := \sum_i m^i \mathbf{v}^i \psi\left(\mathbf{r}^i - \mathbf{x}\right) \tag{2.1b}$$

$$\rho e^h(\mathbf{x},t) := \sum_i \left(\frac{1}{2} m^i \left(\mathbf{v}^i\right)^2 + \phi^i\right) \psi\left(\mathbf{r}^i - \mathbf{x}\right) \tag{2.1c}$$

where m^i, $\mathbf{v}^i$, $\mathbf{r}^i$, and ϕ^i are the mass, velocity, position, and potential energy of atom i. Superscript 'h' represents the thermomechanical expressions of Hardy's approach. The total potential energy of the system $\Phi = \sum_i \phi^i$. The continuum velocity, $\mathbf{v}(\mathbf{x},t)$, is given by

$$\mathbf{v}(\mathbf{x},t) := \rho(\mathbf{x},t)^{-1} \mathbf{p}(\mathbf{x},t) \tag{2.2}$$

The localization function, $\psi(\mathbf{x})$, has the dimension of inverse volume that satisfies $\int_{\mathbb{R}^3} \psi(\mathbf{x}) \mathrm{d}\mathbf{x} = 1$. It can also be proved that

$$\psi\left(\mathbf{r}^i - \mathbf{x}\right) - \psi\left(\mathbf{r}^j - \mathbf{x}\right) = -\mathbf{r}^{ij} \cdot \nabla B\left(\mathbf{x}; \mathbf{r}^i, \mathbf{r}^j\right) \tag{2.3}$$

where $\mathbf{r}^{ij} = \mathbf{r}^i - \mathbf{r}^j$ and the bond function $B(\mathbf{x}; \mathbf{r}^i, \mathbf{r}^j)$ is defined as

$$B\left(\mathbf{x}; \mathbf{r}^i, \mathbf{r}^j\right) := \int_0^1 \psi\left(\lambda \mathbf{r}^{ij} + \mathbf{r}^j - \mathbf{r}\right) \mathrm{d}\lambda \tag{2.4}$$

2.1. Conservation of mass

Taking the partial time derivative of mass density (2.1a) is given by,

$$\frac{\partial \rho(\mathbf{x}, t)}{\partial t} = \sum_i m^i \frac{\partial \psi(\mathbf{r}^i - \mathbf{x})}{\partial t} = \sum_i m^i \frac{\partial \psi(\mathbf{r}^i - \mathbf{x})}{\partial \mathbf{r}^i} \cdot \mathbf{v}^i = -\operatorname{div}\left\{\sum_i m^i \mathbf{v}^i \psi\left(\mathbf{r}^i - \mathbf{x}\right)\right\} = -\operatorname{div}\{\rho \mathbf{v}\} \tag{2.5}$$

It thus can be demonstrated that Hardy's definitions of mass density, momentum density, and velocity obey the continuum conservation of mass.

2.2. Conservation of momentum and stress expression

Taking the partial time derivative of momentum density (2.1b),

$$\begin{aligned}\frac{\partial \mathbf{p}(\mathbf{x}, t)}{\partial t} &= \sum_i m^i \frac{\mathrm{d}\mathbf{v}^i}{\mathrm{d}t} \psi\left(\mathbf{r}^i - \mathbf{x}\right) + m^i \mathbf{v}^i \frac{\partial \psi(\mathbf{r}^i - \mathbf{x})}{\partial t} \\ &= \sum_i \left(\mathbf{f}^i + \mathbf{b}^i\right) \psi\left(\mathbf{r}^i - \mathbf{x}\right) + m^i \mathbf{v}^i \frac{\partial \psi(\mathbf{r}^i - \mathbf{x})}{\partial \mathbf{r}^i} \cdot \mathbf{v}^i\end{aligned} \tag{2.6}$$

where $\mathbf{f}^i = -\frac{\partial \Phi}{\partial \mathbf{r}^i}$ is the interatomic force on atom i, and $\mathbf{b}^i$ represents the body force on atom i from gravity or electromagnetic fields. In the following derivations, body force will be assumed negligible. As discussed in our previous work [34], if we define

$$\mathbf{f}^{ij} := -\frac{\partial \Phi}{\partial \mathbf{r}^{ij}} \tag{2.7}$$

then, $\mathbf{f}^i = -\frac{\partial \Phi}{\partial \mathbf{r}^i} = -\sum_{j \neq i} \frac{\partial \Phi}{\partial \mathbf{r}^{ij}} = \sum_{j \neq i} \mathbf{f}^{ij}$ and $\mathbf{f}^{ij} = -\mathbf{f}^{ji}$ can be established. The right hand side (RHS) of Eq. (2.6) becomes

$$\begin{aligned}&\sum_i \mathbf{f}^i \psi\left(\mathbf{r}^i - \mathbf{x}\right) + m^i \mathbf{v}^i \frac{\partial \psi(\mathbf{r}^i - \mathbf{x})}{\partial \mathbf{r}^i} \cdot \mathbf{v}^i \\ &= \frac{1}{2} \sum_i \sum_{j \neq i} \left(\mathbf{f}^{ij} \psi\left(\mathbf{r}^i - \mathbf{x}\right) + \mathbf{f}^{ji} \psi\left(\mathbf{r}^j - \mathbf{x}\right)\right) - \operatorname{div}\left\{\sum_i m^i \mathbf{v}^i \otimes \mathbf{v}^i \psi\left(\mathbf{r}^i - \mathbf{x}\right)\right\}\end{aligned} \tag{2.8}$$

Using the property of localization function in Eq. (2.3),

$$\begin{aligned}\frac{\partial \mathbf{p}(\mathbf{x}, t)}{\partial t} &= -\frac{1}{2} \sum_i \sum_{j \neq i} \mathbf{f}^{ij} \otimes \mathbf{r}^{ij} \nabla B\left(\mathbf{x}; \mathbf{r}^i, \mathbf{r}^j\right) - \operatorname{div}\left\{\sum_i m^i \mathbf{v}^i \otimes \mathbf{v}^i \psi\left(\mathbf{r}^i - \mathbf{x}\right)\right\} \\ &= \operatorname{div}\left\{-\frac{1}{2} \sum_i \sum_{j \neq i} \mathbf{f}^{ij} \otimes \mathbf{r}^{ij} B\left(\mathbf{x}; \mathbf{r}^i, \mathbf{r}^j\right) - \sum_i m^i \mathbf{v}^i \otimes \mathbf{v}^i \psi\left(\mathbf{r}^i - \mathbf{x}\right)\right\}\end{aligned} \tag{2.9}$$

Hardy defines relative velocity $\tilde{\mathbf{v}}^i(\mathbf{x}, t) := \mathbf{v}^i(t) - \mathbf{v}(\mathbf{x}, t)$. Replacing $\mathbf{v}^i$ with $\tilde{\mathbf{v}}^i$ and $\mathbf{v}$ in Eq. (2.3) (unless otherwise noted, $\mathbf{v}^i$, $\tilde{\mathbf{v}}^i$, and $\mathbf{v}$ represent $\tilde{\mathbf{v}}^i(\mathbf{x}, t)$, $\mathbf{v}^i(t)$, and $\mathbf{v}(\mathbf{x}, t)$ for simplicity),

$$\frac{\partial \mathbf{p}(\mathbf{x}, t)}{\partial t} = \operatorname{div}\left\{-\frac{1}{2} \sum_i \sum_{j \neq i} \mathbf{f}^{ij} \otimes \mathbf{r}^{ij} B\left(\mathbf{x}; \mathbf{r}^i, \mathbf{r}^j\right) - \sum_i m^i \tilde{\mathbf{v}}^i \otimes \tilde{\mathbf{v}}^i \psi\left(\mathbf{r}^i - \mathbf{x}\right) - \rho \mathbf{v} \otimes \mathbf{v}\right\} \tag{2.10}$$

where $\sum_i m^i \tilde{\mathbf{v}}^i \otimes \mathbf{v} \psi(\mathbf{r}^i - \mathbf{x}) = 0$ has been used. From the continuum balance of momentum, we have

$$\frac{\partial \mathbf{p}(\mathbf{x}, t)}{\partial t} = \operatorname{div}\{\boldsymbol{\sigma} - \rho \mathbf{v} \otimes \mathbf{v}\} \tag{2.11}$$

Thus the stress tensor can be identified as

$$\boldsymbol{\sigma} = -\frac{1}{2}\sum_i \sum_{j\neq i} \mathbf{f}^{ij} \otimes \mathbf{r}^{ij} B\left(\mathbf{x}; \mathbf{r}^i, \mathbf{r}^j\right) - \sum_i m^i \tilde{\mathbf{v}}^i \otimes \tilde{\mathbf{v}}^i \psi\left(\mathbf{r}^i - \mathbf{x}\right) \tag{2.12a}$$

$$\boldsymbol{\sigma}_v = -\frac{1}{2}\sum_i \sum_{j\neq i} \mathbf{f}^{ij} \otimes \mathbf{r}^{ij} B\left(\mathbf{x}; \mathbf{r}^i, \mathbf{r}^j\right), \qquad \boldsymbol{\sigma}_k = -\sum_i m^i \tilde{\mathbf{v}}^i \otimes \tilde{\mathbf{v}}^i \psi\left(\mathbf{r}^i - \mathbf{x}\right) \tag{2.12b}$$

The defined quantities satisfy the conservation of momentum. Note that the stress expression is not restricted to two-body potentials and we only use the central force assumption, i.e. $\mathbf{f}^{ij} := -\frac{\partial \Phi}{\partial \mathbf{r}^{ij}}$. A general multibody interatomic potentials can be decomposed into the sum of a two-body term, a three-body term, up to an N-body term [27,35]:

$$\Phi = \frac{1}{2!}\sum_i \sum_{j\neq i} \phi_2\left(r^{ij}\right) + \frac{1}{3!}\sum_i \sum_{j\neq i} \sum_{k\neq i,j} \phi_3\left(r^{ij}, r^{ik}, r^{jk}\right) + \ldots + \frac{1}{N!}\sum_i \sum_{j\neq i} \sum_{k\neq i,j} \cdots \sum_{q\neq i,j,k,\ldots,p} \phi_N\left(r^{ij}, r^{ik}, r^{jk}, \ldots, r^{pq}\right) \tag{2.13a}$$

$$\Phi = \sum_i \phi^i\left(r^{ij}, r^{ik}, r^{jk}, \ldots, r^{pq}\right) \tag{2.13b}$$

where $\phi_N(r^{ij}, r^{ik}, r^{jk}, \ldots, r^{pq})$ represents N-body potential term. There is still no consensus on how to distribute the total energy to individual atoms. A most common way is to evenly distribute the interatomic potential energy to the contributing atoms (Eq. (2.14)), which is reasonable for pair potential systems having the same type of atoms but doubtful for many multibody potentials such as those describing bending and torsional deformations.

$$\phi^i = \frac{1}{2!}\sum_{j\neq i} \phi_2\left(r^{ij}\right) + \frac{1}{3!}\sum_{j\neq i} \sum_{k\neq i,j} \phi_3\left(r^{ij}, r^{ik}, r^{jk}\right) + \ldots + \frac{1}{N!}\sum_{j\neq i} \sum_{k\neq i,j} \cdots \sum_{q\neq i,j,k,\ldots,p} \phi_N\left(r^{ij}, r^{ik}, r^{jk}, \ldots, r^{pq}\right) \tag{2.14}$$

From Eqs. (2.7) and (2.13),

$$\begin{aligned}
\mathbf{f}^{ij} &:= -\frac{\partial \Phi}{\partial \mathbf{r}^{ij}} \\
&= -\frac{1}{2!}\sum_k \sum_{l\neq k} \frac{\partial \phi_2(r^{kl})}{\partial \mathbf{r}^{ij}} - \frac{1}{3!}\sum_k \sum_{l\neq k} \sum_{m\neq k,l} \frac{\partial \phi_3(r^{kl}, r^{km}, r^{lm})}{\partial \mathbf{r}^{ij}} \\
&\quad - \ldots - \frac{1}{N!}\sum_k \sum_{l\neq k} \sum_{m\neq k,l} \cdots \sum_{q\neq k,l,m,\ldots,p} \frac{\partial \phi_N(r^{kl}, r^{km}, r^{lm}, \ldots, r^{pq})}{\partial \mathbf{r}^{ij}} \\
&= -\left(\begin{array}{l} \frac{1}{2!}\sum_k \sum_{l\neq k} \frac{\partial \phi_2}{\partial r^{ij}} (\delta_{ik}\delta_{jl} + \delta_{il}\delta_{jk}) \\ + \frac{1}{3!}\sum_k \sum_{l\neq k} \sum_{m\neq k,l} \frac{\partial \phi_3}{\partial r^{ij}} (\delta_{ik}\delta_{jl} + \delta_{il}\delta_{jk} + \delta_{ik}\delta_{jm} + \delta_{im}\delta_{jk} + \delta_{il}\delta_{jm} + \delta_{im}\delta_{jl}) \\ + \ldots + \frac{1}{N!}\sum_k \sum_{l\neq k} \sum_{m\neq k,l} \cdots \sum_{r\neq k,l,m,\ldots,s} \frac{\partial \phi_N}{\partial r^{ij}} (\delta_{ik}\delta_{jl} + \delta_{il}\delta_{jk} + \ldots + \delta_{is}\delta_{jr} + \delta_{ir}\delta_{js}) \end{array} \right) \frac{\mathbf{r}^{ij}}{r^{ij}} \\
&= \mathbf{f}_2^{ij} + \sum_{k\neq i,j} \mathbf{f}_3^{ij} + \ldots + \frac{N(N-1)}{N!} \sum_{k\neq i,j} \sum_{l\neq i,j,k} \sum_{m\neq i,j,k,l} \cdots \sum_{p\neq k,l,m,\ldots,q} \mathbf{f}_N^{ij}
\end{aligned} \tag{2.15}$$

where $\mathbf{f}_N^{ij} := -\frac{\partial \phi_N}{\partial r^{ij}} \frac{\mathbf{r}^{ij}}{r^{ij}} = -\frac{\partial \phi_N}{\partial \mathbf{r}^{ij}}$ represents the N-body contribution to the central force $\mathbf{f}^{ij}$. Substituting Eq. (2.15) into the expression of $\boldsymbol{\sigma}_v$ in Eq. (2.12b),

$$\boldsymbol{\sigma}_v = -\frac{1}{2}\sum_i \sum_{j\neq i} \left\{ \mathbf{f}_2^{ij} + \sum_{k\neq i,j} \mathbf{f}_3^{ij} + \ldots + \frac{N(N-1)}{N!} \sum_{k\neq i,j} \sum_{l\neq i,j,k} \sum_{m\neq i,j,k,l} \cdots \sum_{p\neq k,l,m,\ldots,q} \mathbf{f}_N^{ij} \right\} \otimes \mathbf{r}^{ij} B\left(\mathbf{x}; \mathbf{r}^i, \mathbf{r}^j\right) \tag{2.16}$$

2.3. Conservation of energy and heat flux expression

We continue the derivation of heat flux expression through the conservation of energy. Taking the partial time derivative of Eq. (2.1c),

$$\frac{\partial (\rho e^h(\mathbf{x}, t))}{\partial t} = \sum_i \left(m^i \mathbf{v}^i \cdot \frac{\mathrm{d}\mathbf{v}^i}{\mathrm{d}t} + \frac{\partial \phi^i}{\partial t} \right) \psi\left(\mathbf{r}^i - \mathbf{x}\right) + \sum_i \left(\frac{1}{2} m^i \left(\mathbf{v}^i\right)^2 + \phi^i \right) \frac{\partial \psi\left(\mathbf{r}^i - \mathbf{x}\right)}{\partial t} \tag{2.17}$$

Similar to the derivation of stress expression, we aim to identify heat flux expression by comparing the balance of energy equations at the atomistic and continuum scales. Therefore, we rewrite the RHS of Eq. (2.17) in a divergence form similar to the continuum energy conservation equation. The second term of the RHS of Eq. (2.17) is

$$\begin{aligned}\sum_i\left(\frac{1}{2}m^i\left(\mathbf{v}^i\right)^2+\phi^i\right)\frac{\partial\psi\left(\mathbf{r}^i-\mathbf{x}\right)}{\partial t}&=-\sum_i\left(\frac{1}{2}m^i\left(\mathbf{v}^i\right)^2+\phi^i\right)\frac{\partial\psi\left(\mathbf{r}^i-\mathbf{x}\right)}{\partial\mathbf{x}}\cdot\mathbf{v}^i\\&=-\operatorname{div}\left\{\sum_i\left(\frac{1}{2}m^i\left(\mathbf{v}^i\right)^2+\phi^i\right)\mathbf{v}^i\psi\left(\mathbf{r}^i-\mathbf{x}\right)\right\}\end{aligned}\tag{2.18}$$

Replacing $\mathbf{v}^i$ by $\tilde{\mathbf{v}}^i$ and $\mathbf{v}$ in Eq. (2.18),

$$\begin{aligned}&\sum_i\left(\frac{1}{2}m^i\left(\mathbf{v}^i\right)^2+\phi^i\right)\frac{\partial\psi\left(\mathbf{r}^i-\mathbf{x}\right)}{\partial t}\\&=\operatorname{div}\left\{-\sum_i m^i\left(\tilde{\mathbf{v}}^i\otimes\tilde{\mathbf{v}}^i\right)\psi\left(\mathbf{r}^i-\mathbf{x}\right)\mathbf{v}-\sum_i\left(\frac{1}{2}m^i\left(\tilde{\mathbf{v}}^i\right)^2+\phi^i\right)\tilde{\mathbf{v}}^i\psi\left(\mathbf{r}^i-\mathbf{x}\right)-\sum_i\left(\frac{1}{2}m^i\left(\mathbf{v}^i\right)^2+\phi^i\right)\psi\left(\mathbf{r}^i-\mathbf{x}\right)\mathbf{v}\right\}\\&=\operatorname{div}\left\{\boldsymbol{\sigma}_k\mathbf{v}-\mathbf{q}_k^h-\rho e^h\mathbf{v}\right\}\end{aligned}\tag{2.19}$$

$$\mathbf{q}_k^h:=\sum_i\left(\frac{1}{2}m^i\left(\tilde{\mathbf{v}}^i\right)^2+\phi^i\right)\tilde{\mathbf{v}}^i\psi\left(\mathbf{r}^i-\mathbf{x}\right)\tag{2.20a}$$

$$\mathbf{q}_{k1}^h:=\sum_i\frac{1}{2}m^i\left(\tilde{\mathbf{v}}^i\right)^2\tilde{\mathbf{v}}^i\psi\left(\mathbf{r}^i-\mathbf{x}\right)\tag{2.20b}$$

$$\mathbf{q}_{k2}^h:=\sum_i\phi^i\tilde{\mathbf{v}}^i\psi\left(\mathbf{r}^i-\mathbf{x}\right)\tag{2.20c}$$

The first term of the RHS of Eq. (2.17) can also be arranged in a divergence form as:

$$\begin{aligned}\sum_i\left(m^i\mathbf{v}^i\cdot\frac{\mathrm{d}\mathbf{v}^i}{\mathrm{d}t}+\frac{\partial\phi^i}{\partial t}\right)\psi\left(\mathbf{r}^i-\mathbf{x}\right)&=\sum_i\left(\mathbf{f}^i\cdot\mathbf{v}^i+\frac{1}{2}\sum_j\sum_{k\neq j}\frac{\partial\phi^i}{\partial\mathbf{r}^{jk}}\cdot\left(\mathbf{v}^j-\mathbf{v}^k\right)\right)\psi\left(\mathbf{r}^i-\mathbf{x}\right)\\&=\sum_i\left(-\sum_{j\neq i}\sum_k\frac{\partial\phi^k}{\partial\mathbf{r}^{ij}}\cdot\mathbf{v}^i+\frac{1}{2}\sum_j\sum_{k\neq j}\frac{\partial\phi^i}{\partial\mathbf{r}^{jk}}\cdot\left(\mathbf{v}^j-\mathbf{v}^k\right)\right)\psi\left(\mathbf{r}^i-\mathbf{x}\right)\\&=\sum_i\sum_{j\neq i}\sum_{k\neq i}\left(\frac{\partial\phi^k}{\partial\mathbf{r}^{ij}}\cdot\mathbf{v}^i\right)\mathbf{r}^{ik}\cdot\nabla B\left(\mathbf{x};\mathbf{r}^i,\mathbf{r}^k\right)\\&=\operatorname{div}\left\{\sum_i\sum_{j\neq i}\sum_{k\neq i}\left(\frac{\partial\phi^j}{\partial\mathbf{r}^{ik}}\cdot\mathbf{v}^i\right)\mathbf{r}^{ij}B\left(\mathbf{x};\mathbf{r}^i,\mathbf{r}^j\right)\right\}\end{aligned}\tag{2.21}$$

Replacing $\mathbf{v}^i$ by $\tilde{\mathbf{v}}^i$ and $\mathbf{v}$ in Eq. (2.21),

$$\begin{aligned}\sum_i\left(m^i\mathbf{v}^i\cdot\frac{\mathrm{d}\mathbf{v}^i}{\mathrm{d}t}+\frac{\partial\phi^i}{\partial t}\right)\psi\left(\mathbf{r}^i-\mathbf{x}\right)&=\operatorname{div}\left\{\sum_i\sum_{j\neq i}\sum_{k\neq i}\frac{\partial\phi^j}{\partial\mathbf{r}^{ik}}\cdot\left(\tilde{\mathbf{v}}^i+\mathbf{v}\right)\mathbf{r}^{ij}B\left(\mathbf{x};\mathbf{r}^i,\mathbf{r}^j\right)\right\}\\&=\operatorname{div}\left\{\sum_i\sum_{j\neq i}\sum_{k\neq i}\frac{\partial\phi^j}{\partial\mathbf{r}^{ik}}\otimes\mathbf{r}^{ij}B\left(\mathbf{x};\mathbf{r}^i,\mathbf{r}^j\right)\mathbf{v}-\mathbf{q}_v^h\right\}\end{aligned}\tag{2.22}$$

$$\mathbf{q}_v^h:=-\sum_i\sum_{j\neq i}\sum_{k\neq i}\left(\frac{\partial\phi^j}{\partial\mathbf{r}^{ik}}\cdot\tilde{\mathbf{v}}^i\right)\mathbf{r}^{ij}B\left(\mathbf{x};\mathbf{r}^i,\mathbf{r}^j\right)\tag{2.23}$$

In order for the continuum conservation of energy satisfied by the defined thermomechanical quantities, $\sum_i\sum_{j\neq i}\sum_{k\neq i}\frac{\partial\phi^j}{\partial\mathbf{r}^{ik}}\otimes\mathbf{r}^{ij}B\left(\mathbf{x};\mathbf{r}^i,\mathbf{r}^j\right)=\boldsymbol{\sigma}_v$ needs to be established. Note that for pair potentials,

$$\sum_i\sum_{j\neq i}\sum_{k\neq i}\frac{\partial\phi^j}{\partial\mathbf{r}^{ik}}\otimes\mathbf{r}^{ij}B\left(\mathbf{x};\mathbf{r}^i,\mathbf{r}^j\right)=\sum_i\sum_{j\neq i}\frac{\partial\phi^j}{\partial\mathbf{r}^{ij}}\otimes\mathbf{r}^{ij}B\left(\mathbf{x};\mathbf{r}^i,\mathbf{r}^j\right)$$

$$= \frac{1}{2}\sum_i \sum_{j\neq i} \phi_2'(r^{ij})\hat{\mathbf{r}}^{ij} \otimes \mathbf{r}^{ij} B(\mathbf{x}; \mathbf{r}^i, \mathbf{r}^j)$$
$$= -\frac{1}{2}\sum_i \sum_{j\neq i} \mathbf{f}^{ij} \otimes \mathbf{r}^{ij} B(\mathbf{x}; \mathbf{r}^i, \mathbf{r}^j) = \boldsymbol{\sigma}_v \tag{2.24}$$

where $\hat{\mathbf{r}}^{ij}$ is the unit vector in the direction of $\mathbf{r}^{ij}$. For embedded-atom method, we have $\phi^i = F_i(\sum_{j\neq i}\rho_j(r^{ij})) + \frac{1}{2}\sum_{j\neq i}\varphi(r^{ij})$,

$$\sum_i \sum_{j\neq i}\sum_{k\neq i} \frac{\partial \phi^j}{\partial \mathbf{r}^{ik}} \otimes \mathbf{r}^{ij} B(\mathbf{x}; \mathbf{r}^i, \mathbf{r}^j) = \sum_i \sum_{j\neq i} \left(F_j'\rho_i'(r^{ij}) + \frac{1}{2}\varphi'(r^{ij})\right)\hat{\mathbf{r}}^{ij} \otimes \mathbf{r}^{ij} B(\mathbf{x}; \mathbf{r}^i, \mathbf{r}^j)$$
$$= \frac{1}{2}\sum_i \sum_{j\neq i} \left(F_i'\rho_j'(r^{ij}) + F_j'\rho_i'(r^{ij}) + \varphi'(r^{ij})\right)\hat{\mathbf{r}}^{ij} \otimes \mathbf{r}^{ij} B(\mathbf{x}; \mathbf{r}^i, \mathbf{r}^j)$$
$$= -\frac{1}{2}\sum_i \sum_{j\neq i} \mathbf{f}^{ij} \otimes \mathbf{r}^{ij} B(\mathbf{x}; \mathbf{r}^i, \mathbf{r}^j) = \boldsymbol{\sigma}_v \tag{2.25}$$

However, for general multibody potentials,

$$\sum_i \sum_{j\neq i}\sum_{k\neq i} \frac{\partial \phi^j}{\partial \mathbf{r}^{ik}} \otimes \mathbf{r}^{ij} B(\mathbf{x}; \mathbf{r}^i, \mathbf{r}^j) \neq -\frac{1}{2}\sum_i \sum_{j\neq i} \mathbf{f}^{ij} \otimes \mathbf{r}^{ij} B(\mathbf{x}; \mathbf{r}^i, \mathbf{r}^j) = \boldsymbol{\sigma}_v \tag{2.26}$$

Therefore, from Eqs. (2.17)–(2.23) and (2.26), it can be shown that

$$\frac{\partial(\rho e^h(\mathbf{x}, t))}{\partial t} \neq \operatorname{div}\{\boldsymbol{\sigma}\mathbf{v} - \mathbf{q}^h - e^h\mathbf{v}\} \tag{2.27}$$

Thus the derived thermomechanical expressions for multibody potential do not necessarily satisfy the continuum conservation laws. This may arise from the manner in which the total potential energy is distributed among the atoms. Intuitively, total interatomic energy describing bending and torsional deformation should not be distributed evenly among the atoms, neither should the distribution factor be constant with time. However, we will demonstrate in Section 4 that the conservation of energy is not significantly violated by such derived Hardy's thermomechanical quantities for multibody potentials. Using Eq. (2.15), the heat flux expression obtained from Hardy's approach is

$$\mathbf{q}^h = \sum_i \left(\frac{1}{2}m^i(\tilde{\mathbf{v}}^i)^2 + \phi^i\right)\tilde{\mathbf{v}}^i \psi(\mathbf{r}^i - \mathbf{x})$$
$$+ \sum_i \sum_{j\neq i}\left(\frac{1}{2}\mathbf{f}_2^{ij} + \frac{1}{3}\sum_{k\neq i,j}(\mathbf{f}_3^{ij} + \mathbf{f}_3^{ik}) + \frac{N-1}{N!}\sum_{k\neq i,j}\cdots\sum_{q\neq i,j,k,\ldots,p}(\mathbf{f}_N^{ij} + (N-2)\mathbf{f}_N^{ik})\right)\cdot\tilde{\mathbf{v}}^i\mathbf{r}^{ij}B(\mathbf{x}; \mathbf{r}^i, \mathbf{r}^j) \tag{2.28}$$

where we have used

$$\sum_{k\neq i}\frac{\partial\phi^j}{\partial\mathbf{r}^{ik}} = \frac{1}{2!}\sum_{k\neq i}\sum_{l\neq j}\frac{\partial\phi_2(r^{jl})}{\partial\mathbf{r}^{ik}}\delta_{il}\delta_{jk} + \frac{1}{3!}\sum_{k\neq i}\sum_{l\neq j}\sum_{m\neq j,l}\frac{\partial\phi_3(r^{jl}, r^{jm}, r^{lm})}{\partial\mathbf{r}^{ik}}(\delta_{il}\delta_{jk} + \delta_{im}\delta_{jk} + \delta_{il}\delta_{km} + \delta_{im}\delta_{kl}) + \ldots$$
$$+ \frac{1}{N!}\sum_{k\neq i}\sum_{l\neq j}\sum_{m\neq j,l}\cdots\sum_{r\neq j,k,\ldots,s}\frac{\partial\phi_N(r^{jl}, r^{jm}, r^{lm}, \ldots, r^{rs})}{\partial\mathbf{r}^{ik}}(\delta_{il}\delta_{jk} + \delta_{im}\delta_{jk} + \ldots + \delta_{iq}\delta_{jk} + \ldots$$
$$+ \delta_{ir}\delta_{ks} + \delta_{is}\delta_{kr})$$
$$= \frac{1}{2!}\frac{\partial\phi_2(r^{ij})}{\partial\mathbf{r}^{ij}} + \frac{2}{3!}\sum_{k\neq i,j}\left(\frac{\partial\phi_3(r^{ji}, r^{jk}, r^{ik})}{\partial\mathbf{r}^{ij}} + \frac{\partial\phi_3(r^{ji}, r^{jk}, r^{ik})}{\partial\mathbf{r}^{ik}}\right) + \ldots$$
$$+ \frac{N-1}{N!}\sum_{k\neq i,j}\sum_{l\neq i,j,k}\sum_{m\neq i,j,k,l}\cdots\sum_{p\neq i,j,k,l,\ldots,q}\left(\frac{\partial\phi_N(r^{ji}, r^{jk}, r^{ik}, \ldots, r^{pq})}{\partial\mathbf{r}^{ij}}\right.$$
$$\left.+ (N-2)\frac{\partial\phi_N(r^{ji}, r^{jk}, r^{ik}, \ldots, r^{pq})}{\partial\mathbf{r}^{ik}}\right) \tag{2.29}$$

3. Admal & Tadmor's heat flux expression

An alternative way is to avoid defining energy density directly but to propose heat flux expression applicable to multi-body potentials and deriving the energy density expression that satisfies the conservation of energy. The resulting expression of heat flux does not have the terms involving individual atomic potential thus avoids the ambiguities of distributing total interatomic potential among the atoms. Admal and Tadmor [33] adopted Murdoch's approach [30] and developed the expressions of heat flux vector and energy density convenient to compute from MD results.

We review the derivation of heat flux vector in the original Admal & Tadmor's methodology [33] briefly. In their work, Irving–Kirkwood procedure was reformatted by incorporating Murdoch's methodology so that the resulting expressions for the internal energy density and heat flux are no longer restricted to pair potential systems. Rather than defining mass and momentum density in terms of the localization function, the densities are defined based on the probability density function $W(\mathbf{r}^1,\ldots,\mathbf{r}^N;\mathbf{v}^1,\ldots,\mathbf{v}^N)$ in the original Admal & Tadmor's approach:

$$\rho(\mathbf{x},t) := \sum_i m^i \int_{\mathbb{R}^{3N}\times\mathbb{R}^{3N}} W\,\delta\left(\mathbf{r}^i-\mathbf{x}\right)\mathrm{d}\mathbf{r}^1\mathrm{d}\mathbf{r}^2\ldots\mathrm{d}\mathbf{r}^N\mathrm{d}\mathbf{v}^1\mathrm{d}\mathbf{v}^2\ldots\mathrm{d}\mathbf{v}^N \tag{3.1}$$

With the property of the Dirac delta distribution function,

$$\begin{aligned}\rho(\mathbf{x},t) &= \sum_i m^i \int_{\mathbb{R}^{3N}\times\mathbb{R}^{3N}} W\,\mathrm{d}\mathbf{r}^1\ldots\mathrm{d}\mathbf{r}^{i-1}\mathrm{d}\mathbf{r}^{i+1}\ldots\mathrm{d}\mathbf{r}^N\mathrm{d}\mathbf{v}^1\mathrm{d}\mathbf{v}^2\ldots\mathrm{d}\mathbf{v}^N\\ &:= \sum_i m^i\left\langle W\,|\mathbf{r}^i=\mathbf{x}\right\rangle\end{aligned} \tag{3.2}$$

where $\langle W|\mathbf{r}^i=\mathbf{x}\rangle$ denotes that $\mathbf{r}^i$ is substituted with $\mathbf{x}$ in W, and the integral of W is taken over all its arguments but $\mathbf{r}^i$. Similarly, the momentum and kinetic energy density are defined as:

$$\mathbf{p}(\mathbf{x},t) := \sum_i m^i\left\langle \mathbf{v}^i W\,|\mathbf{r}^i=\mathbf{x}\right\rangle \tag{3.3}$$

$$\rho e_k(\mathbf{x},t) := \frac{1}{2}\sum_i m^i\left\langle (\mathbf{v}^i)^2 W\,|\mathbf{r}^i=\mathbf{x}\right\rangle \tag{3.4}$$

Taking partial time derivative of Eq. (3.4),

$$\begin{aligned}\frac{\partial(\rho e_k)}{\partial t} &= \sum_i m^i\left\langle (\mathbf{v}^i)^2\frac{\partial W}{\partial t}\,\middle|\,\mathbf{r}^i=\mathbf{x}\right\rangle\\ &= \frac{1}{2}\sum_i m^i\left\langle (\mathbf{v}^i)^2\sum_{j=1}\left(-\mathbf{v}^j\cdot\nabla_{\mathbf{r}^j}W+\frac{\nabla_{\mathbf{r}^j}\Phi}{m^j}\cdot\nabla_{\mathbf{v}^j}W\right)\,\middle|\,\mathbf{r}^i=\mathbf{x}\right\rangle\end{aligned} \tag{3.5}$$

where Liouville's theorem that describes the evolution of the probability density function is applied:

$$\frac{\partial W}{\partial t}+\sum_{i=1}\left(\mathbf{v}^i\cdot\nabla_{\mathbf{r}^i}W-\frac{\nabla_{\mathbf{r}^i}\Phi}{m^i}\cdot\nabla_{\mathbf{v}^i}W\right)=0 \tag{3.6}$$

With the identity $\int_{\mathbb{R}^3}\mathbf{G}\cdot\nabla_{\mathbf{r}^i}W\,\mathrm{d}\mathbf{r}^i=-\int_{\mathbb{R}^3}W\,\mathrm{div}_{\mathbf{r}^i}\mathbf{G}\mathrm{d}\mathbf{r}^i$, where $\mathbf{G}$ is any continuously differentiable vector or tensor-valued function defined on the phase space and satisfies certain additional decay conditions described in Admal and Tadmor [36], one can find that $\langle(\mathbf{v}^i)^2\mathbf{v}^j\cdot\nabla_{\mathbf{r}^j}W\,|\mathbf{r}^i=\mathbf{x}\rangle=0$ for $i\neq j$; from another identity $\int_{\mathbb{R}^3}\mathbf{G}\cdot\nabla_{\mathbf{v}^i}W\,\mathrm{d}\mathbf{v}^i=-\int_{\mathbb{R}^3}W\,\mathrm{div}_{\mathbf{v}^i}\mathbf{G}\mathrm{d}\mathbf{v}^i$, $\langle(\mathbf{v}^i)^2\frac{\nabla_{\mathbf{r}^j}\Phi}{m^j}\cdot\nabla_{\mathbf{v}^j}W\,|\mathbf{r}^i=\mathbf{x}\rangle=0$ for $i\neq j$. Therefore Eq. (3.5) becomes

$$\frac{\partial(\rho e_k)}{\partial t}=-\frac{1}{2}\sum_i m^i\left\langle (\mathbf{v}^i)^2\mathbf{v}^i\cdot\nabla_{\mathbf{r}^i}W\,|\mathbf{r}^i=\mathbf{x}\right\rangle-\frac{1}{2}\sum_i\left\langle (\mathbf{v}^i)^2\mathbf{f}^i\cdot\nabla_{\mathbf{v}^i}W\,|\mathbf{r}^i=\mathbf{x}\right\rangle \tag{3.7}$$

Replacing $\mathbf{v}^i$ by $\tilde{\mathbf{v}}^i$ and $\mathbf{v}$ in Eq. (3.7), the first term becomes

$$\begin{aligned}&-\frac{1}{2}\sum_i m^i\left\langle (\mathbf{v}^i)^2\mathbf{v}^i\cdot\nabla_{\mathbf{r}^j}W\,|\mathbf{r}^i=\mathbf{x}\right\rangle\\ &\quad=-\mathrm{div}\left\{\sum_i m^i\left\langle(\tilde{\mathbf{v}}^i\otimes\tilde{\mathbf{v}}^i)W\,|\mathbf{r}^i=\mathbf{x}\right\rangle\mathbf{v}+\sum_i\frac{1}{2}m^i\left\langle(\tilde{\mathbf{v}}^i)^2\tilde{\mathbf{v}}^i W\,|\mathbf{r}^i=\mathbf{x}\right\rangle+\sum_i\frac{1}{2}m^i\left\langle(\mathbf{v}^i)^2 W\,|\mathbf{r}^i=\mathbf{x}\right\rangle\mathbf{v}\right\}\end{aligned} \tag{3.8}$$

With

$$\boldsymbol{\sigma}_k := -\sum_i m^i \langle (\tilde{\mathbf{v}}^i \otimes \tilde{\mathbf{v}}^i) W \,|\mathbf{r}^i = \mathbf{x}\rangle \tag{3.9}$$

$$\mathbf{q}_k := \sum_i \frac{1}{2} m^i \langle (\tilde{\mathbf{v}}^i)^2 \tilde{\mathbf{v}}^i W \,|\mathbf{r}^i = \mathbf{x}\rangle \tag{3.10}$$

Eq. (3.8) becomes

$$-\frac{1}{2}\sum_i m^i \langle (\mathbf{v}^i)^2 \mathbf{v}^i \cdot \nabla_{\mathbf{r}^i} W \,|\mathbf{r}^i = \mathbf{x}\rangle = \operatorname{div}\{\boldsymbol{\sigma}_k \mathbf{v} - \mathbf{q}_k - \rho e_k \mathbf{v}\} \tag{3.11}$$

Applying $\int_{\mathbb{R}^3} \mathbf{G} \cdot \nabla_{\mathbf{v}^i} W \,\mathrm{d}\mathbf{v}^i = -\int_{\mathbb{R}^3} W \operatorname{div}_{\mathbf{v}^i} \mathbf{G} \mathrm{d}\mathbf{v}^i$ to the second term of Eq. (3.7)

$$\begin{aligned} -\frac{1}{2}\sum_i \langle (\mathbf{v}^i)^2 \mathbf{f}^i \cdot \nabla_{\mathbf{v}^i} W \,|\mathbf{r}^i = \mathbf{x}\rangle &= \frac{1}{2}\sum_i \langle \operatorname{div}_{\mathbf{v}^i} \{\mathbf{f}^i (\mathbf{v}^i)^2\} W \,|\mathbf{r}^i = \mathbf{x}\rangle = \sum_i \langle \mathbf{f}^i \cdot \mathbf{v}^i W \,|\mathbf{r}^i = \mathbf{x}\rangle \\ &= \sum_i \langle \mathbf{f}^i \cdot \tilde{\mathbf{v}}^i W \,|\mathbf{r}^i = \mathbf{x}\rangle + \sum_i \langle \mathbf{f}^i W \,|\mathbf{r}^i = \mathbf{x}\rangle \cdot \mathbf{v} \\ &= \sum_i \langle \mathbf{f}^i \cdot \tilde{\mathbf{v}}^i W \,|\mathbf{r}^i = \mathbf{x}\rangle + \operatorname{div} \boldsymbol{\sigma}_v \cdot \mathbf{v} \end{aligned} \tag{3.12}$$

where $\mathbf{v}^i = \tilde{\mathbf{v}}^i + \mathbf{v}$ and $\operatorname{div} \boldsymbol{\sigma}_v = \sum_i \langle \mathbf{f}^i W |\mathbf{r}^i = \mathbf{x}\rangle \cdot \mathbf{v}$ is applied.

Now the key step is to decompose $\sum_i \langle \mathbf{f}^i \cdot \tilde{\mathbf{v}}^i W |\mathbf{r}^i = \mathbf{x}\rangle$ into $-\operatorname{div} \mathbf{q}_v$ and $\bar{g}_s(\mathbf{x}, t)$. For further details, interested reader is referred to Admal and Tadmor [33].

$$\mathbf{q}_v := \frac{1}{2}\sum_{i\neq j} \int_{z\in\mathbb{R}^3} z \int_{s=0}^{1} \left\langle \mathbf{f}^{ij} \cdot \left(\frac{\mathbf{v}^i + \mathbf{v}^j}{2} - \mathbf{v}\right) W \,\middle|\, \mathbf{r}^i = \mathbf{x} + s\mathbf{z}, \mathbf{r}^j = \mathbf{x} - (1-s)\mathbf{z} \right\rangle \mathrm{d}s\mathrm{d}\mathbf{z} \tag{3.13}$$

$$\bar{g}_s := \frac{1}{2}\sum_{i\neq j} \langle \mathbf{f}^{ij} \cdot (\mathbf{v}^i - \mathbf{v}^j) W \,|\mathbf{r}^i = \mathbf{x}\rangle \tag{3.14}$$

$\mathbf{q}$ is defined as

$$\mathbf{q} := \mathbf{q}_k + \mathbf{q}_v \tag{3.15}$$

To satisfy the energy conservation, e_v can be obtained as

$$e_v = \int_0^t \frac{1}{\rho} (\boldsymbol{\sigma} : \nabla_{\mathbf{x}} \mathbf{v} - \bar{g}_s(\mathbf{x}, t)) dt + c \tag{3.16}$$

Further spatial averaging is applied to the thermomechanical expressions when calculation is made on MD simulation results. The probability density function, W, is taken as $W^{MD}(\mathbf{r}^1, \ldots, \mathbf{r}^N; \mathbf{v}^1, \ldots, \mathbf{v}^N) = \prod_i \delta(\mathbf{r}^i - \mathbf{r}^i_{MD}(t)) \delta(\mathbf{v}^i - \mathbf{v}^i_{MD}(t))$ due to the deterministic nature of typical MD simulations. The spatial averaged thermomechanical field, $f_\psi(\mathbf{x}, t)$, from the Irving–Kirkwood point-wise field, $f(\mathbf{y}, t; W)$, is given by

$$f_\psi(\mathbf{x}, t) = \int_{\mathbb{R}^3} \psi(\mathbf{y} - \mathbf{x}) f(\mathbf{y}, t; W) \mathrm{d}\mathbf{y} \tag{3.17}$$

where $f(\mathbf{y}, t; W)$ is obtained from the previous procedures. Applying Eq. (3.17) to Eqs. (3.10), (3.13) and (3.16),

$$\mathbf{q}_{\psi,k} := \sum_i \frac{1}{2} m^i (\tilde{\mathbf{v}}^i_{\psi,MD})^2 \tilde{\mathbf{v}}^i_{\psi,MD} \psi(\mathbf{r}^i_{MD} - \mathbf{x}) \tag{3.18}$$

$$\begin{aligned} \mathbf{q}_{\psi,v} &= \frac{1}{2}\sum_{i\neq j} \int_{\mathbb{R}^3\times\mathbb{R}^3} \left\langle \mathbf{f}^{ij} \cdot \left(\frac{\mathbf{v}^i + \mathbf{v}^j}{2} - \mathbf{v}\right) W^{MD} \,\middle|\, \mathbf{r}^i = \mathbf{u}, \mathbf{r}^j = \mathbf{v} \right\rangle (\mathbf{u} - \mathbf{v}) B(\mathbf{x}; \mathbf{u}, \mathbf{v}) \mathrm{d}\mathbf{u}\mathrm{d}\mathbf{v} \\ &= \frac{1}{2}\sum_{i\neq j} \mathbf{f}^{ij}_{MD} \cdot \left(\frac{\mathbf{v}^i_{MD} + \mathbf{v}^j_{MD}}{2} - \mathbf{v}_\psi\right) (\mathbf{x}^i_{MD} - \mathbf{x}^j_{MD}) B(\mathbf{x}; \mathbf{x}^i_{MD}, \mathbf{x}^j_{MD}) \end{aligned} \tag{3.19}$$

$$e^{AT}_{\psi,v} = \int_0^t \frac{1}{\rho} (\boldsymbol{\sigma}_\psi : \nabla_{\mathbf{x}} \mathbf{v}_\psi - \bar{g}_{\psi,s}(\mathbf{x}, t)) dt + c \tag{3.20}$$

$$\boldsymbol{\sigma}_{\psi} = -\sum_i m^i \left(\tilde{\mathbf{v}}^i_{\psi,MD} \otimes \tilde{\mathbf{v}}^i_{\psi,MD}\right) \psi\left(\mathbf{r}^i_{MD} - \mathbf{x}\right) - \frac{1}{2}\sum_{i\neq j} \mathbf{f}^{ij}_{MD} \otimes \left(\mathbf{x}^i_{MD} - \mathbf{x}^j_{MD}\right) B\left(\mathbf{x}; \mathbf{x}^i_{MD}, \mathbf{x}^j_{MD}\right) \tag{3.21}$$

$$\bar{g}_{\psi,s}(\mathbf{x},t) = \frac{1}{2}\sum_{i\neq j} \mathbf{f}^{ij}_{MD} \cdot \left(\mathbf{v}^i_{MD} - \mathbf{v}^j_{MD}\right) \psi\left(\mathbf{r}^i_{MD} - \mathbf{x}\right) \tag{3.22}$$

where $\tilde{\mathbf{v}}^i_{\psi,MD} := \mathbf{v}^i_{MD} - \mathbf{v}_{\psi}$.

The most significant difference of Admal & Tadmor's methodology from Hardy's is that the potential part of energy density is not explicitly defined, apart from the ensemble averaging employed in Admal & Tadmor's expressions. We here use similar methodology in Admal & Tadmor's work. However, we apply spatial averaging directly through the localization function, $\psi(\mathbf{x},t)$, instead of ensemble averaging through the probability density function followed by spatial averaging. Besides the mass density and momentum density, only the kinetic energy density is defined as follows,

$$\rho e^{AT}_k(\mathbf{x},t) := \sum_i \frac{1}{2} m^i \left(\mathbf{v}^i\right)^2 \psi\left(\mathbf{r}^i - \mathbf{x}\right) \tag{3.23}$$

Superscript '*AT*' represents the thermomechanical expressions of Admal & Tadmor's approach. Since the derivation of stress tensor from the conservation of momentum is identical to that from Hardy's approach, we only focus on the derivation of heat flux vector and potential energy density.

Taking the partial time derivative of kinetic energy density Eq. (3.23),

$$\frac{\partial\left(\rho e^{AT}_k(\mathbf{x},t)\right)}{\partial t} = \sum_i m^i \mathbf{v}^i \cdot \frac{\mathrm{d}\mathbf{v}^i}{\mathrm{d}t} \psi\left(\mathbf{r}^i - \mathbf{x}\right) + \sum_i \frac{1}{2} m^i \left(\mathbf{v}^i\right)^2 \frac{\partial \psi\left(\mathbf{r}^i - \mathbf{x}\right)}{\partial t} \tag{3.24}$$

The second term of the RHS of Eq. (3.24) is

$$\begin{aligned}\sum_i \frac{1}{2} m^i \left(\mathbf{v}^i\right)^2 \frac{\partial \psi\left(\mathbf{r}^i - \mathbf{x}\right)}{\partial t} &= -\sum_i \frac{1}{2} m^i \left(\mathbf{v}^i\right)^2 \frac{\partial \psi\left(\mathbf{r}^i - \mathbf{x}\right)}{\partial \mathbf{x}} \cdot \mathbf{v}^i \\ &= -\operatorname{div}\left\{\sum_i \frac{1}{2} m^i \left(\mathbf{v}^i\right)^2 \mathbf{v}^i \psi\left(\mathbf{r}^i - \mathbf{x}\right)\right\}\end{aligned} \tag{3.25}$$

Replacing $\mathbf{v}^i$ by $\tilde{\mathbf{v}}^i$ and $\mathbf{v}$ in Eq. (3.25),

$$\begin{aligned}&\sum_i \frac{1}{2} m^i \left(\mathbf{v}^i\right)^2 \frac{\partial \psi\left(\mathbf{r}^i - \mathbf{x}\right)}{\partial t} \\ &= \operatorname{div}\left\{-\sum_i m^i \left(\tilde{\mathbf{v}}^i \otimes \tilde{\mathbf{v}}^i\right) \psi\left(\mathbf{r}^i - \mathbf{x}\right)\mathbf{v} - \sum_i \frac{1}{2} m^i \left(\tilde{\mathbf{v}}^i\right)^2 \tilde{\mathbf{v}}^i \psi\left(\mathbf{r}^i - \mathbf{x}\right) - \sum_i \frac{1}{2} m^i \left(\mathbf{v}^i\right)^2 \psi\left(\mathbf{r}^i - \mathbf{x}\right)\mathbf{v}\right\} \\ &= \operatorname{div}\left\{\boldsymbol{\sigma}_k \mathbf{v} - \mathbf{q}^{AT}_k - \rho e^{AT}_k \mathbf{v}\right\}\end{aligned} \tag{3.26}$$

$$\mathbf{q}^{AT}_k := \sum_i \frac{1}{2} m^i \left(\tilde{\mathbf{v}}^i\right)^2 \tilde{\mathbf{v}}^i \psi\left(\mathbf{r}^i - \mathbf{x}\right) \tag{3.27}$$

Note that the $\mathbf{q}^{AT}_k$ is the same with $\mathbf{q}^h_{k1}$ from Eq. (2.20b), and the term involving the atomic potential energy (Eq. (2.20c)) in Hardy's heat flux expression does not appear here. The first term of the RHS of Eq. (3.24) is

$$\begin{aligned}\sum_i m^i \mathbf{v}^i \cdot \frac{\mathrm{d}\mathbf{v}^i}{\mathrm{d}t} \psi\left(\mathbf{r}^i - \mathbf{x}\right) &= \sum_i \sum_{j\neq i} \mathbf{f}^{ij} \cdot \mathbf{v}^i \psi\left(\mathbf{r}^i - \mathbf{x}\right) \\ &= \sum_i \sum_{j\neq i} \mathbf{f}^{ij} \cdot \tilde{\mathbf{v}}^i \psi\left(\mathbf{r}^i - \mathbf{x}\right) + \sum_i \sum_{j\neq i} \mathbf{f}^{ij} \psi\left(\mathbf{r}^i - \mathbf{x}\right) \cdot \mathbf{v} \\ &= \sum_i \sum_{j\neq i} \mathbf{f}^{ij} \cdot \tilde{\mathbf{v}}^i \psi\left(\mathbf{r}^i - \mathbf{x}\right) + \operatorname{div} \boldsymbol{\sigma}_v \cdot \mathbf{v}\end{aligned} \tag{3.28}$$

From Eqs. (3.24), (3.26), and (3.28), we have

$$\frac{\partial\left(\rho e^{AT}_k(\mathbf{x},t)\right)}{\partial t} = \operatorname{div}\left\{\boldsymbol{\sigma}_k \mathbf{v} - \mathbf{q}^{AT}_k - \rho e^{AT}_k \mathbf{v}\right\} + \sum_i \sum_{j\neq i} \mathbf{f}^{ij} \cdot \tilde{\mathbf{v}}^i \psi\left(\mathbf{r}^i - \mathbf{x}\right) + \operatorname{div} \boldsymbol{\sigma}_v \cdot \mathbf{v} \tag{3.29}$$

We now propose the potential part of heat flux expression the same with Hardy's original expression for pair potentials [17] and that in Admal & Tadmor's work [33].

$$\mathbf{q}_v^{AT} := \frac{1}{2}\sum_i\sum_{j\neq i}\mathbf{f}^{ij}\cdot\tilde{\mathbf{v}}^i B\left(\mathbf{x};\mathbf{r}^i,\mathbf{r}^j\right) = \frac{1}{2}\sum_i\sum_{j\neq i}\mathbf{f}^{ij}\cdot\left(\frac{\mathbf{v}^i+\mathbf{v}^j}{2}-\mathbf{v}\right)B\left(\mathbf{x};\mathbf{r}^i,\mathbf{r}^j\right) \tag{3.30}$$

To satisfy the conservation of energy, the expression of the potential part of energy density can be derived as below. Eq. (3.29) can be reformatted as

$$\frac{\partial\rho}{\partial t}e_k^{AT}+\rho\frac{\partial e_k^{AT}}{\partial t} = -\operatorname{div}\mathbf{q}_k^{AT}+\operatorname{div}\boldsymbol{\sigma}\cdot\mathbf{v}+\boldsymbol{\sigma}_k:\nabla\mathbf{v}-\rho\nabla e_k^{AT}\cdot\mathbf{v}-e_k^{AT}\operatorname{div}\{\rho\mathbf{v}\}+\sum_i\sum_{j\neq i}\mathbf{f}^{ij}\cdot\tilde{\mathbf{v}}^i\psi\left(\mathbf{r}^i-\mathbf{x}\right) \tag{3.31}$$

Applying the conservation of mass $\frac{\partial\rho}{\partial t}=-\operatorname{div}\{\rho\mathbf{v}\}$ and the conservation of momentum $\rho\frac{\mathrm{d}\mathbf{v}}{\mathrm{d}t}=\operatorname{div}\boldsymbol{\sigma}$ to Eq. (3.31),

$$\rho\frac{\mathrm{d}\tilde{e}_k^{AT}}{\partial t} = -\operatorname{div}\mathbf{q}_k^{AT}+\boldsymbol{\sigma}_k:\nabla\mathbf{v}+\sum_i\sum_{j\neq i}\mathbf{f}^{ij}\cdot\tilde{\mathbf{v}}^i\psi\left(\mathbf{r}^i-\mathbf{x}\right) \tag{3.32}$$

where

$$\tilde{e}_k^{AT} := e_k^{AT}-\frac{1}{2}\mathbf{v}^2 \tag{3.33}$$

The balance of energy requires

$$\rho\frac{\mathrm{d}\tilde{e}}{\partial t} = \boldsymbol{\sigma}:\nabla_{\mathbf{x}}\mathbf{v}-\operatorname{div}\mathbf{q} \tag{3.34}$$

where

$$\tilde{e} := e-\frac{1}{2}\mathbf{v}^2 \tag{3.35}$$

Subtracting Eq. (3.32) from Eq. (3.34),

$$\begin{aligned}\rho\frac{\mathrm{d}e_v^{AT}}{\partial t} &= \boldsymbol{\sigma}_v:\nabla_{\mathbf{x}}\mathbf{v}-\operatorname{div}\mathbf{q}_v^{AT}-\sum_i\sum_{j\neq i}\mathbf{f}^{ij}\cdot\tilde{\mathbf{v}}^i\psi\left(\mathbf{r}^i-\mathbf{x}\right)\\ &= -\frac{1}{2}\sum_i\sum_{j\neq i}\mathbf{f}^{ij}\cdot\left(\mathbf{v}^i-\mathbf{v}^j\right)\psi\left(\mathbf{r}^i-\mathbf{x}\right)\end{aligned} \tag{3.36}$$

$$e_v^{AT} = -\int_0^t\frac{1}{2\rho}\sum_i\sum_{j\neq i}\mathbf{f}^{ij}\cdot\left(\mathbf{v}^i-\mathbf{v}^j\right)\psi\left(\mathbf{r}^i-\mathbf{x}\right)\mathrm{d}t+c \tag{3.37}$$

Comparing Eqs. (3.18), (3.19) and (3.20) with Eqs. (3.27), (3.30) and (3.37), it is easy to see that the potential energy density expressions are different from the direct spatial averaging expressions in our modified approach, but the heat flux expressions remain the same. It is worth mentioning that another heat flux expression derived in a similar manner can be found in Murdoch's work, where $\mathbf{q}^M$ is defined as

$$\begin{aligned}\mathbf{q}^M(\mathbf{x}) := &\sum_i\frac{1}{2}m^i\left(\tilde{\mathbf{v}}^i\right)^2\tilde{\mathbf{v}}^i\psi\left(\mathbf{r}^i-\mathbf{x}\right)\\ &+\frac{1}{2}\int_{\mathbb{R}^3}\mathbf{z}\int_0^1\sum_i\sum_{j\neq i}\left(\mathbf{f}^{ij}\cdot\tilde{\mathbf{v}}^i(\mathbf{x}+s\mathbf{z})+\mathbf{f}^{ij}\tilde{\mathbf{v}}^j\left(\mathbf{x}-(1-s)\mathbf{z}\right)\right)\psi\left(\mathbf{x}+s\mathbf{z}-\mathbf{r}^i\right)\psi\left(\mathbf{x}-(1-s)\mathbf{z}-\mathbf{r}^j\right)\mathrm{d}s\mathrm{d}\mathbf{z}\end{aligned} \tag{3.38}$$

However, this expression is more difficult to implement in MD simulations. Using Eq. (2.15), the heat flux expression obtained from this alternative approach is

$$\begin{aligned}\mathbf{q}^{AT} = &\sum_i\frac{1}{2}m^i\left(\tilde{\mathbf{v}}^i\right)^2\tilde{\mathbf{v}}^i\psi\left(\mathbf{r}^i-\mathbf{x}\right)\\ &+\frac{1}{2}\sum_i\sum_{j\neq i}\left(\mathbf{f}_2^{ij}+\sum_{k\neq i,j}\mathbf{f}_3^{ij}+\ldots+\frac{N(N-1)}{N!}\sum_{k\neq i,j}\sum_{l\neq i,j,k}\sum_{m\neq i,j,k,l}\cdots\sum_{p\neq k,l,m,\ldots,q}\mathbf{f}_N^{ij}\right)\cdot\tilde{\mathbf{v}}^i\mathbf{r}^{ij}B\left(\mathbf{x};\mathbf{r}^i,\mathbf{r}^j\right)\end{aligned} \tag{3.39}$$

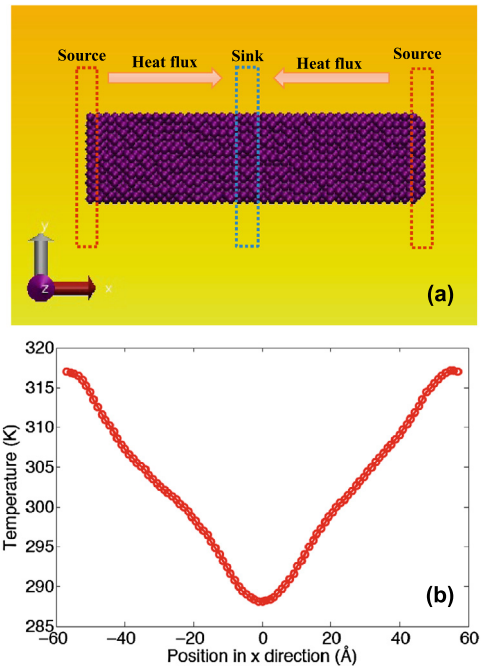

Fig. 1. (a) Nonequilibrium molecular dynamics (NEMD) model to impose the constant heat flux along the x direction, and (b) temperature profile within the iron crystal after heat transfer is switched on for 1000 ps.

4. Molecular dynamic simulations

In this section, we compare the two expressions of the heat flux vector (Eqs. (2.28) and (3.39)) using constant heat flux MD simulations of two distinctive systems: crystalline iron and amorphous PE polymer. The constant heat flux is imposed along the x direction of both systems by adding a constant amount of kinetic energy, ΔE_k, per time step to the source region and subtracting from the sink region (Fig. 1(a)) [37,38]. Total momentum of the source or sink region are conserved during the addition or subtraction of energy. With the prescribed $\Delta E_k/\delta t$, where δt is the time interval, the magnitude of the heat flux in the x direction is given by:

$$q_x = \frac{\Delta E_k}{2A\delta t} \tag{4.1}$$

where A is the cross sectional area. Since we consider steady non-equilibrium conditions here, time averaging [39] is applied to investigate the convergence of the heat flux, which is computed every 100 time steps (0.1 ps). All the MD simulations are performed using LAMMPS [40] with a timestep size of 1 fs. The localization function ψ (Eq. (4.2)) is chosen to be

$$\psi(r) = \begin{cases} c & \text{if } r \le R_c - \delta \\ \frac{1}{2}c\left(1 - \cos\left(\frac{R_c - r}{\delta}\pi\right)\right) & \text{if } R_c - \delta < r \le R_c \\ 0 & \text{otherwise} \end{cases} \tag{4.2}$$

where $c = 1/4\pi\left(\frac{1}{6}R_c^3 + \frac{1}{6}(R_c-\delta)^3 - \frac{\delta^2}{\pi^2}(2R_c-\delta)\right)$ is used to keep $\psi(r)$ normalized. It is easy to verify that $\psi(R_c-\delta) = c$, $\psi(R_c) = 0$, and $\psi'(R_c-\delta) = \psi'(R_c) = 0$, so that the C^1 nature of $\psi(r)$ is satisfied, i.e., $\psi(r)$ is continuously differentiable. The value of δ can be varied to control the fraction of the spatial averaging volume that has the constant value c. The change of the localization function with δ can be found in Fig. 2. We test the conservation of energy numerically using the computed mass density (Eq. (2.1a)), energy density (Eqs. (2.1c), (3.23), (3.37)), velocity (Eq. (2.2)), stress (Eq. (2.12)), and heat flux (Eqs. (2.28) and (3.39)) [41,42]. Discretized version of Eq. (3.34) is given by

$$\rho\frac{\tilde{e}^{(j+1)} - \tilde{e}^{(j)}}{\delta t} + \rho\left\{\frac{\tilde{e}^{(i+1)} - \tilde{e}^{(i)}}{\delta x}v_x + \frac{\tilde{e}^{(k+1)} - \tilde{e}^{(k)}}{\delta y}v_y + \frac{\tilde{e}^{(m+1)} - \tilde{e}^{(m)}}{\delta z}v_z\right\}$$
$$= \begin{bmatrix} \sigma_{xx} & \sigma_{xy} & \sigma_{xz} \\ \sigma_{yx} & \sigma_{yy} & \sigma_{yz} \\ \sigma_{zx} & \sigma_{zy} & \sigma_{zz} \end{bmatrix} : \begin{bmatrix} \frac{v_x^{(i+1)} - v_x^{(i)}}{\delta x} & \frac{v_x^{(k+1)} - v_x^{(k)}}{\delta y} & \frac{v_x^{(m+1)} - v_x^{(m)}}{\delta z} \\ \frac{v_y^{(i+1)} - v_y^{(i)}}{\delta x} & \frac{v_y^{(k+1)} - v_y^{(k)}}{\delta y} & \frac{v_y^{(m+1)} - v_y^{(m)}}{\delta z} \\ \frac{v_z^{(i+1)} - v_z^{(i)}}{\delta x} & \frac{v_z^{(k+1)} - v_z^{(k)}}{\delta y} & \frac{v_z^{(m+1)} - v_z^{(m)}}{\delta z} \end{bmatrix}$$

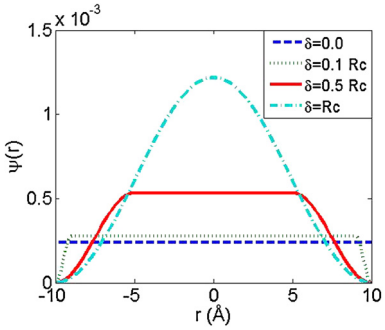

Fig. 2. Spatial averaging function $\psi(r)$ (Eq. (4.2)) with varying δ at $R_c = 10$ Å.

$$-\left(\frac{q_x^{(i+1)} - q_x^{(i)}}{\delta x} + \frac{q_y^{(k+1)} - q_y^{(k)}}{\delta y} + \frac{q_z^{(m+1)} - q_z^{(m)}}{\delta z}\right) \tag{4.3}$$

Here, $\boldsymbol{\sigma}_{xx}^{(ikmj)}$ represents $\boldsymbol{\sigma}_{xx}(x_i, y_k, z_m, t_j)$ and similarly for $\rho^{(ikmj)}$ and $\mathbf{v}^{(ikmj)}(v_\alpha^{(ikmj)})$. For simplicity, superscripts are not explicitly written at (x_i, y_k, z_m, t_j) if not necessary. For example, $\boldsymbol{\sigma}_{xx}^{((i+1)kmj)}$ is written as $\boldsymbol{\sigma}_{xx}^{(i+1)}$. $\delta x = x_{i+1} - x_i$, $\delta y = y_{k+1} - y_k$, $\delta z = z_{m+1} - z_m$, and $\delta t = t_{j+1} - t_j$. δt is chosen to be 0.1 fs and $\delta x = \delta y = \delta z = 0.05$ Å. The mass density, energy density, velocity, stress, and heat flux are computed in terms of atomic variables at chosen spatial points (x_i, y_k, z_m) and time instance, t_j. The agreement between the two sides of the balance laws is tested by plotting the left hand side (LHS) and right hand side (RHS) of the equations. Throughout this paper, LHS of the balance of energy is presented in solid line while RHS in dashed line.

4.1. Calculation of heat flux in the crystalline iron

The iron crystal has the dimension of $L_x = 40[100]$, $L_y = 5[010]$, and $L_z = 5[001]$ in the x, y, and z directions (Fig. 1(a)). Periodic boundary conditions are applied to all directions and EAM potential is used to describe the atomic interaction. The system is first equilibrated at around 300 K for 1000 ps under *NPT* condition with $P = 0$ GPa and $T = 300$ K, followed by a further equilibration as an *NVE* ensemble for 100 ps. A constant amount of kinetic energy per time step is then added to/subtracted from the heat control regions which have the length of 3 lattice in the x direction. $\Delta E_k/\delta t$ is specified to be 3 eV ps^{-1}, so q_x is 29.6 nW nm^{-2} from Eq. (4.1). After equilibration under $N\mathbf{q}V$ condition for 1000 ps, a steady temperature field (Fig. 1(b)) can be established and the data of atomic position and velocity is collected afterwards. Since the temperature distribution generally follows a linear manner (Fig. 1(b)), the temperature gradient can be estimated through a linear fitting ($\delta T/\delta x \approx 0.56$ K Å^{-1}). With the prescribed heat flux q_x, thermal conductivity can be calculated by Fourier's law as 5.29 W m^{-1} K^{-1}. The estimated thermal conductivity is much lower than experimental reported values (70–80 W m^{-1} K^{-1}) [43], resulted from the missing electronic degree of freedom in classical MD simulations.

Fig. 3 shows the validity of energy balance of the computed thermomechanical quantities by plotting the LHS and RHS of Eq. (4.3). δ is chosen as R_c. Both Hardy's and Admal & Tadmor's approaches show good agreements between two sides of Eq. (4.3) regardless of the spatial averaging size R_c. We choose 5 continuum spatial points on the cross section locating at the negative x away from the heat control region to investigate the convergence of computed heat flux, so q_x have positive values due to the symmetric temperature gradient with respect to x.

The effects of time averaging window size and spatial window size are shown in Fig. 4. Hardy's and Admal & Tadmor's heat flux almost overlap with each other. Even though the difference between Hardy's and Admal & Tadmor's heat flux is not significant in this specific example, it cannot be generalized to all EAM potential systems. It is also worth mentioning that the main contribution to the total heat flux is the potential part in both Hardy's and Admal & Tadmor's heat flux expressions. When the spatial averaging radius R_c is small, significant discrepancies can be found between the values of single spatial point and averaged values from 5 spatial points. Heat fluxes in three directions get close to but not exactly converged to the expected values. Heat flux curves become smooth after averaging over 200 ps. At $R_c = 4$ Å, q_x fluctuates around 21.1 nW nm^{-2} for the randomly chosen single point and 25.4 nW nm^{-2} after averaging over 5 points at $\delta = 0.1R_c$, obviously lower than the expected value 29.6 nW nm^{-2}. In comparison, $\delta = R_c$ gives better estimation, with q_x fluctuating around 24.2 nW nm^{-2} for the randomly chosen single point and 28.8 nW nm^{-2} after averaging over 5 points, which falls within 3% from the expected value. The influence of the specific form of localization function by varying δ cannot be observed at larger spatial averaging volume ($R_c = 7$ and 10 Å). At $R_c = 7$ Å, the averaged values from 5 points are 31.0 (30.6) and 29.8 (29.8) nW nm^{-2} using Hardy's and Admal & Tadmor's heat flux expressions, respectively (the values computed with $\delta = R_c$ are in parentheses). At $R_c = 10$ Å, the averaged values from 5 points are 31.5 (31.7) and 30.4 (30.7) nW nm^{-2} using Hardy's and Admal & Tadmor's heat flux expressions, respectively. The largest discrepancy 31.7 nW nm^{-2} is 7% from the expected values. It seems that Admal & Tadmor's heat flux expression gives slightly better predictions in this case.

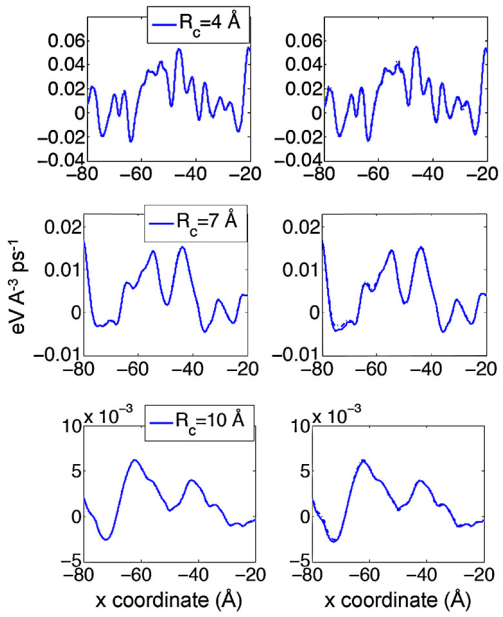

Fig. 3. Balance of energy using Hardy's (left column) and Admal & Tadmor's (right column) approaches with varying spatial averaging volume R_c for the iron crystal modeled by EAM potential, where the LHS of the balance of energy is presented in solid line while RHS in dashed line.

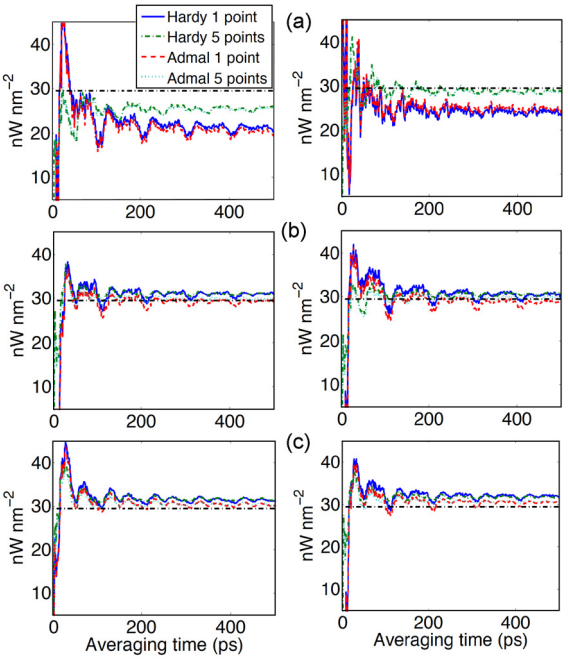

Fig. 4. Convergence of q_x with respect to averaging time window at (a) $R_c = 4$ Å, (b) $R_c = 7$ Å and (c) $R_c = 10$ Å in the iron crystal with $\delta = 0.1R_c$ (left column) and $\delta = R_c$ (right column).

4.2. Calculation of heat flux in the PE polymer

We proceed to compute the heat flux in the PE polymer. A CG PE model described by multibody potentials [44,45] (Table 1) is established. The interatomic potential of the CG PE polymer employed here is composed of two-body terms (stretching and non-bonded interaction), three-body term (bending interaction), and four-body term (torsional interaction). The specific form of the central force for the CG PE model involving four-body potentials to compute the stress (Eq. (2.16)) and heat flux (Eqs. (2.28) and (3.39)) can be found in our previous studies [34]. Details of the CG model have been described in other studies [44–47], thus only some main features are mentioned here for completeness. Each CH_2 is treated

Table 1
Functional form and parameters of the force field for the CG PE.

Type of interaction	Potential form and parameters	
Stretching	$\phi_{stretch} = k_b(r - r_0)^2$ $k_b = 2000\ \mathrm{kJ\,mol^{-1}\,\AA^{-2}}$, $l_{eq} = 1.53$ Å	(4.4a)
Bending	$\phi_{bend} = k_\theta(\cos\theta - \cos\theta_0)^2$ $k_\theta = 520\ \mathrm{kJ\,mol^{-1}}$, $\theta_0 = 112.813°$	(4.4b)
Torsional	$\phi_{torsion} = c_0 + c_1\cos\varphi + c_2\cos^2\varphi + c_3\cos^3\varphi + c_4\cos^4\varphi$ $c_0 = 8.832\ \mathrm{kJ\,mol^{-1}}$, $c_1 = 18.087\ \mathrm{kJ\,mol^{-1}}$, $c_2 = 4.88\ \mathrm{kJ\,mol^{-1}}$, $c_3 = -31.8\ \mathrm{kJ\,mol^{-1}}$	(4.4c)
Non-bonded	$\phi_{LJ} = 4\varepsilon\left[\left(\frac{\sigma}{r}\right)^{12} - \left(\frac{\sigma}{r}\right)^{6}\right]$ $\varepsilon/k_B = 57$ K, $\boldsymbol{\sigma} = 4.28$ Å, k_B is Boltzmann constant	(4.4d)

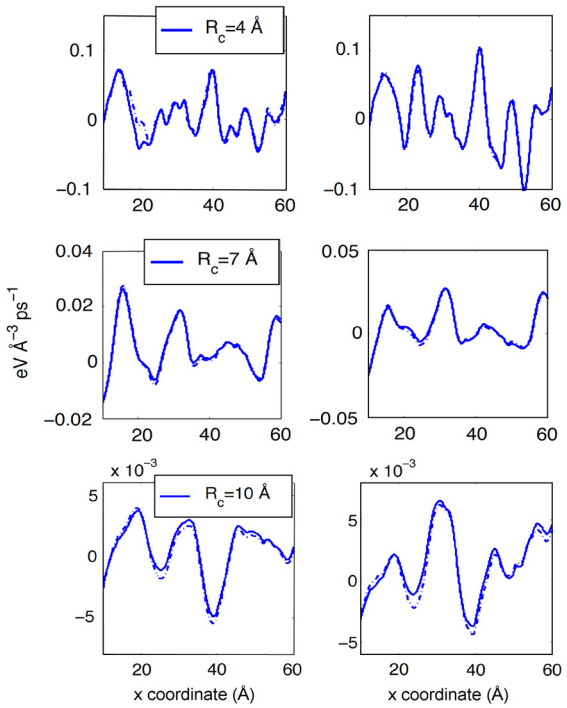

Fig. 5. Balance of energy using Hardy's (left column) and Admal & Tadmor's (right column) approaches with varying spatial averaging volume R_c for the PE polymer, where the LHS of the balance of energy is presented in solid line while RHS in dashed line.

as a superatom, having a mass of 14 u. The CH_3 group at the end of the chain is represented by the same superatom. 100 PE polymer chain each having 100 superatoms is generated at 500 K using the excluded volume method [48], with an initial density of around 0.5 $\mathrm{g\,cm^{-3}}$. The excluded volume method [48] guarantees that the generated PE configuration is energetically preferable. The PE polymer samples as prepared are relaxed under *NPT* condition for 500 ps at 300 K and with an applied isotropic zero pressure using MD simulation. The PE system has the dimension of $L_x = 288.2$ Å, $L_y = 33.6$ Å, and $L_z = 33.6$ Å at 300 K. In order to establish a constant heat flux condition within the system, kinetic energy is added to/subtracted from heat control regions which have the length of 100 Å in the x direction. $\Delta E_k/\delta t$ is specified to be 4.34 $\mathrm{eV\,ps^{-1}}$, so q_x is 26.7 $\mathrm{nW\,nm^{-2}}$ from Eq. (4.1). After an equilibration under the $N\mathbf{q}V$ condition for 1000 ps, a steady temperature field can be established and the data of atomic position and velocity is collected afterwards. The temperature gradient is approximately 15.2 $\mathrm{K\,\AA^{-1}}$. The thermal conductivity can be calculated by Fourier's law as 0.17 $\mathrm{W\,m^{-1}\,K^{-1}}$ with the prescribed heat flux q_x, falling in the range of the reported values (0.1–0.4 $\mathrm{W\,m^{-1}\,K^{-1}}$) [49–51].

Fig. 5 shows the validity of energy conservation of the computed thermomechanical quantities by plotting the LHS and RHS of Eq. (4.3). δ is chosen as R_c. Even though Hardy's approach has been proved not to strictly obey the conservation of energy theoretically in Section 2, the discrepancy between the two sides of Eq. (4.3) is not significant. Thus the balance of energy is not much violated, especially at large spatial averaging volume. Again, the main contribution to the total heat flux is the potential part in both Hardy's and Admal & Tadmor's heat flux expressions.

The convergence of heat flux is demonstrated in Fig. 6. Up to 5 continuum spatial points are chosen on the cross section locating at the positive x away from the heat control region, so q_x have negative values due to the symmetric temperature

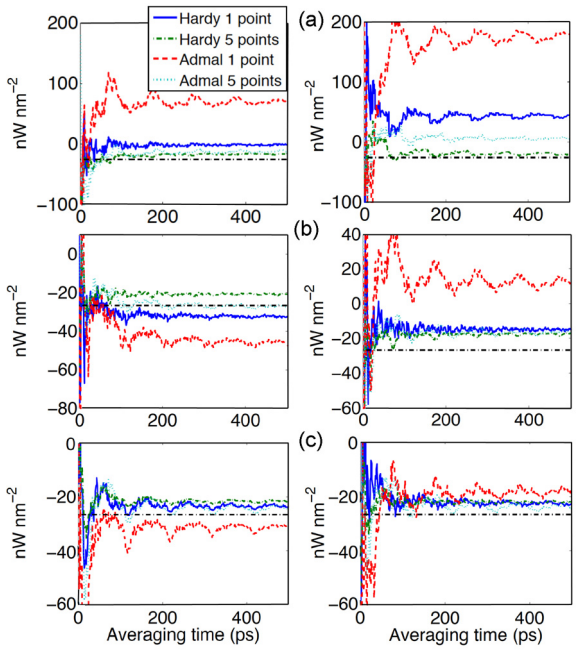

Fig. 6. Convergence of q_x with respect to averaging time window at (a) $R_c = 4$ Å, (b) $R_c = 7$ Å and (c) $R_c = 10$ Å in the PE polymer with $\delta = 0.1R_c$ (left column) and $\delta = R_c$ (right column).

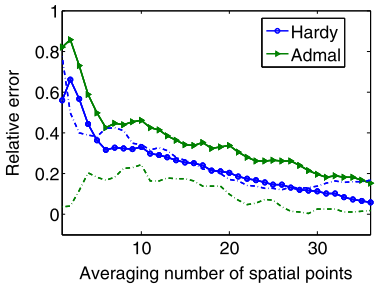

Fig. 7. Relative error of the averaged heat flux in the PE system with the averaging number of spatial points at $R_c = 10$ Å and $\delta = 0.1R_c$ (averaged values with 500 ps and 200 ps time window size are represented in solid lines and dashed lines, respectively).

gradient with respect to x. In contrast to the iron crystal simulated by EAM potential, we observe obviously different results from Hardy's and Admal & Tadmor's heat flux expressions. Averaging over multiple spatial points is essential to provide more accurate predictions of the expected values at $R_c = 4$ and 7 Å. The influence of the specific form of localization function is more pronounced for the PE polymer compared with the iron crystal. At small and moderate averaging volume, $\delta = 0.1R_c$ tends to give better estimation of the averaged values over 5 points. When $R_c = 4$ Å, averaged heat flux converges to -17.8 (-21.2) and -12.6 (-5.3) nW nm^{-2} using Hardy's and Admal & Tadmor's heat flux approaches, respectively (the values computed with $\delta = R_c$ are in parentheses). At $R_c = 7$ Å, heat flux converges to -21.0 (-17.8) and -27.0 (-16.5) nW nm^{-2} using Hardy's and Admal & Tadmor's heat flux approaches, respectively. The approximations at $R_c = 10$ Å are improved on average, and the discrepancies between the two approaches also reduce noticeably. However, largest divergence from the expected values can still be as much as 38%.

More spatial points are chosen on the same cross section in order to investigate the convergence of the computed heat flux with averaging number of points (Fig. 7). The computed heat flux for the PE polymer slowly converges to the system averaged value with increasing number of spatial points. As the number of points reaches 30, the relative error of the heat flux computed from Hardy's and Admal & Tadmor's expressions fluctuates around 3%. Even though a smaller time averaging window size (200 ps) can provide a satisfying estimation with Admal & Tadmor's approach in this case, larger time averaging window size (up to 500 ps) is recommended given that the convergence using both approaches can be improved.

5. Conclusions

In this study, we derive continuum heat flux expressions from atomistic quantities for the systems modeled by multi-body potentials, based on existent theories on calculating continuum thermomechanical quantities from the atomistic scale.

The original Hardy's expressions for pair potential systems are extended by defining the central force between two atoms for most practical multibody potentials and distributing the total interatomic potential energy evenly among the contributing atoms. We also modify Admal & Tadmor's approach by implementing only spatial averaging through the localization function. In the theoretical derivation, Hardy's thermomechanical quantities have not been found to obey the conservation of energy exactly for general multibody systems. On the other hand, an integration over time appears in the definition of energy density to satisfy the continuum conservation law in Admal & Tadmor's approach.

The derived heat flux expressions are applied to a crystalline iron modeled by EAM potential and an amorphous PE polymer modeled by stretching, bending, torsional, and non-bonded potentials. The computed heat fluxes are compared with the expected system averaged values in constant heat flux MD simulations. Proper size of the spatial and temporal averaging window as well as the specific forms of the localization function are investigated. For the non-equilibrium systems at steady state considered here, lower thresholds of both the spatial and temporal window size are recommended for computing the continuum heat flux fields but may be different for various systems [20]. At smaller spatial averaging volume, the computed heat flux can vary significantly with the specific forms of localization function, and also need longer time to converge (up to 500 ps). With relatively large averaging volume, a time window size of 200–300 ps enables convergence. Hardy's and Admal & Tadmor's approaches give comparable averaged values with respect to the expected system values in most cases. However, the predictions for the PE polymer using the same number of spatial averaging points are worse than that for iron crystal, which should be ascribed to the distinctive atomistic structures of the two systems: the crystalline iron has much more uniform lattice structure compared with the amorphous PE polymer. A further study of the heat flux fields in the PE polymer reveals that over 30 spatial points as well as a large time averaging window size (500 ps) is necessary for a good estimation of the system averaged value.

Acknowledgement

The authors gratefully acknowledge the support of the Office of Naval Research under Grant N00014-13-1-0386.

References

[1] D. Frenkel, B. Smit, Understanding Molecular Simulation, Computational Science Series, Academic, New York, 2001.
[2] J.M. Haile, Molecular Dynamics Simulation Elementary Methods, Wiley, New York, 1992.
[3] D.C. Rapaport, The Art of Molecular Dynamics Simulation, Cambridge University Press, London, 2004.
[4] C.J. Kimmer, R.E. Jones, Continuum constitutive models from analytical free energies, J. Phys. Condens. Matter 19 (2007) 326207.
[5] P.A. Klein, J.A. Zimmerman, Coupled atomistic–continuum simulations using arbitrary overlapping domains, J. Comput. Phys. 213 (2006) 86–116.
[6] V.B. Shenoy, R. Miller, E.B. Tadmor, D. Rodney, R. Phillips, M. Ortiz, An adaptive finite element approach to atomic-scale mechanics—the quasicontinuum method, J. Mech. Phys. Solids 47 (1999) 611–642.
[7] E.B. Tadmor, M. Ortiz, R. Phillips, Quasicontinuum analysis of defects in solids, Philos. Mag. A 73 (1996) 1529–1563.
[8] R.E. Rudd, J.Q. Broughton, Concurrent coupling of length scales in solid state systems, Phys. Status Solidi B 217 (2000) 251–291.
[9] L.E. Shilkrot, R.E. Miller, W.A. Curtin, Multiscale plasticity modeling: coupled atomistics and discrete dislocation mechanics, J. Mech. Phys. Solids 52 (2004) 755–787.
[10] S.P. Xiao, T. Belytschko, A bridging domain method for coupling continua with molecular dynamics, Comput. Methods Appl. Mech. Eng. 193 (2004) 1645–1669.
[11] J. Knap, M. Ortiz, An analysis of the quasicontinuum method, J. Mech. Phys. Solids 49 (2001) 1899–1923.
[12] W. E, B. Engquist, X. Li, W. Ren, E. Vanden-Eijnden, Heterogeneous multiscale methods: a review, Commun. Comput. Phys. 2 (2007) 367–450.
[13] R. Clausius, XVI. On a mechanical theorem applicable to heat, Philos. Mag. Ser. 4 40 (1870) 122–127.
[14] J.C. Maxwell, On reciprocal figures, frames and diagrams of forces, Trans. R. Soc. Edinb. XXVI (1870) 1–43.
[15] J.C. Maxwell, Van der Waals on the continuity of the gaseous and liquid states, Nature 10 (1874) 477–480.
[16] J.H. Irving, J.G. Kirkwood, The statistical mechanical theory of transport processes. IV. The equations of hydrodynamics, J. Chem. Phys. 18 (1950) 817–829.
[17] R.J. Hardy, Formulas for determining local properties in molecular-dynamics simulations: shock waves, J. Chem. Phys. 76 (1982) 622–628.
[18] S. Root, R.J. Hardy, D.R. Swanson, Continuum predictions from molecular dynamics simulations: shock waves, J. Chem. Phys. 118 (2003) 3161–3165.
[19] R.E. Jones, J.A. Zimmerman, J. Oswald, T. Belytschko, An atomistic J-integral at finite temperature based on Hardy estimates of continuum fields, J. Phys. Condens. Matter 23 (2011) 015002.
[20] H.U. Manfred, K.M. Kranthi, P. Panayiotis, On the estimation of spatial averaging volume for determining stress using atomistic methods, Model. Simul. Mater. Sci. Eng. 21 (2013) 015010.
[21] J.A. Zimmerman, R.E. Jones, J.A. Templeton, A material frame approach for evaluating continuum variables in atomistic simulations, J. Comput. Phys. 229 (2010) 2364–2389.
[22] J.A. Zimmerman, E.B. Webb III, J.J. Hoyt, R.E. Jones, P.A. Klein, D.J. Bammann, Calculation of stress in atomistic simulation, Model. Simul. Mater. Sci. Eng. 12 (2004) S319.
[23] Y. Chen, Local stress and heat flux in atomistic systems involving three-body forces, J. Chem. Phys. 124 (2006) 054113.
[24] J. Tersoff, New empirical model for the structural properties of silicon, Phys. Rev. Lett. 56 (1986) 632.
[25] J. Tersoff, Modeling solid-state chemistry: interatomic potentials for multicomponent systems, Phys. Rev. B 39 (1989) 5566(R).
[26] F.H. Stillinger, T.A. Weber, Computer simulation of local order in condensed phases of silicon, Phys. Rev. B 31 (1985) 5262.
[27] T.J. Delph, Conservation laws for multibody interatomic potentials, Model. Simul. Mater. Sci. Eng. 13 (2005) 585.
[28] A.I. Murdoch, The motivation of continuum concepts and relations from discrete considerations, Q. J. Mech. Appl. Math. 36 (1983) 163–187.
[29] A.I. Murdoch, D. Bedeaux, On the physical interpretation of fields in continuum mechanics, Int. J. Eng. Sci. 31 (1993) 1345–1373.
[30] A.I. Murdoch, D. Bedeaux, Continuum equations of balance via weighted averages of microscopic quantities, Proc. R. Soc. Lond. Ser. A, Math. Phys. Sci. 445 (1994) 157–179.
[31] A. Ian Murdoch, On the microscopic interpretation of stress and couple stress, in: C.-S. Man, R. Fosdick (Eds.), The Rational Spirit in Modern Continuum Mechanics, Springer, Netherlands, 2004, pp. 599–625.
[32] A.I. Murdoch, A critique of atomistic definitions of the stress tensor, J. Elast. 88 (2007) 113–140.

[33] N.C. Admal, E.B. Tadmor, Stress and heat flux for arbitrary multibody potentials: a unified framework, J. Chem. Phys. 134 (2011) 184106.
[34] Y. Fu, J.-H. Song, On computing stress in polymer systems involving multi-body potentials from molecular dynamics simulation, J. Chem. Phys. 141 (2014) 054108.
[35] J.W. Martin, Many-body forces in metals and the Brugger elastic constants, J. Phys. C, Solid State Phys. 8 (1975) 2837.
[36] N. Admal, E.B. Tadmor, A unified interpretation of stress in molecular systems, J. Elast. 100 (2010) 63–143.
[37] T. Ikeshoji, B. Hafskjold, Non-equilibrium molecular dynamics calculation of heat conduction in liquid and through liquid–gas interface, Mol. Phys. 81 (1994) 251–261.
[38] E.B. Webb, J.A. Zimmerman, S.C. Seel, Reconsideration of continuum thermomechanical quantities in atomic scale simulations, Math. Mech. Solids 13 (2008) 221–266.
[39] Y. Fu, A.C. To, On the evaluation of Hardy's thermomechanical quantities using ensemble and time averaging, Model. Simul. Mater. Sci. Eng. 21 (2013) 055015.
[40] http://lammps.sandia.gov/.
[41] Y. Fu, A.C. To, A modification to Hardy's thermomechanical theory for conserving fundamental properties more accurately: tensile and shear failures in iron, Model. Simul. Mater. Sci. Eng. 22 (2014) 015010.
[42] Y. Fu, A.C. To, A modification to Hardy's thermomechanical theory that conserves fundamental properties more accurately, J. Appl. Phys. 113 (2013) 233505.
[43] CRC Handbook of Chemistry and Physics, William M. Haynes (Editor in Chief), 95th edition, 2014.
[44] D. Brown, J.H.R. Clarke, Molecular dynamics simulation of an amorphous polymer under tension. 1. Phenomenology, Macromolecules 24 (1991) 2075–2082.
[45] F.M. Capaldi, M.C. Boyce, G.C. Rutledge, Molecular response of a glassy polymer to active deformation, Polymer 45 (2004) 1391–1399.
[46] Y. Li, M. Kröger, W.K. Liu, Nanoparticle geometrical effect on structure, dynamics and anisotropic viscosity of polyethylene nanocomposites, Macromolecules 45 (2012) 2099–2112.
[47] Y. Fu, J.-H. Song, Large deformation mechanism of glassy polyethylene polymer nanocomposites: coarse grain molecular dynamics study, Comput. Mater. Sci. 96 (2014) 485–494.
[48] J.I. McKechnie, D. Brown, J.H.R. Clarke, Methods of generating dense relaxed amorphous polymer samples for use in dynamic simulations, Macromolecules 25 (1992) 1562–1567.
[49] C.L. Choy, Y.W. Wong, G.W. Yang, T. Kanamoto, Elastic modulus and thermal conductivity of ultradrawn polyethylene, J. Polym. Sci., Part B, Polym. Phys. 37 (1999) 3359–3367.
[50] A. Henry, G. Chen, High thermal conductivity of single polyethylene chains using molecular dynamics simulations, Phys. Rev. Lett. 101 (2008) 235502.
[51] Sheng Shen, A. Henry, J. Tong, R. Zheng, G. Chen, Polyethylene nanofibres with very high thermal conductivities, Nat. Nanotechnol. 5 (2010) 251–255.